TECHNICAL REPORT BRL-TR-3214

BRL

AN ANALYSIS ON THE STABILITY OF THE MIE-GRÜNEISEN EQUATION OF STATE FOR DESCRIBING THE BEHAVIOR OF SHOCK-LOADED MATERIALS

STEVEN B. SEGLETES

MARCH 1991

U.S. ARMY LABORATORY COMMAND

BALLISTIC RESEARCH LABORATORY
ABERDEEN PROVING GROUND, MARYLAND

NOTICES

Destroy this report when it is no longer needed. DO NOT return it to the originator.

Additional copies of this report may be obtained from the National Technical Information Service, U.S. Department of Commerce, 5285 Port Royal Road, Springfield, VA 22161.

The findings of this report are not to be construed as an official Department of the Army position, unless so designated by other authorized documents.

The use of trade names or manufacturers' names in this report does not constitute indorsement of any commercial product.

UNCLASSIFIED

REPORT DOCUMENTATION PAGE

Form Approved
OMB No. 0704-0188

1. AGENCY USE ONLY (Leave blank)	2. REPORT DATE	3. REPORT TYPE AND DATES COVERED
	March 1991	Final Jun 89 - Sep 90

4. TITLE AND SUBTITLE

An Analysis on the Stability of the Mie-Grüneisen Equation of State for Describing the Behavior of Shock-Loaded Materials

5. FUNDING NUMBERS

PR: 1L162618AH80
WO: 44592-012-26-6201

6. AUTHOR(S)

Steven B. Segletes

7. PERFORMING ORGANIZATION NAME(S) AND ADDRESS(ES)

8. PERFORMING ORGANIZATION REPORT NUMBER

9. SPONSORING / MONITORING AGENCY NAME(S) AND ADDRESS(ES)

US Army Ballistic Research Laboratory
ATTN: SLCBR-DD-T
Aberdeen Proving Ground, MD 21005-5066

10. SPONSORING / MONITORING AGENCY REPORT NUMBER

BRL-TR-3214

11. SUPPLEMENTARY NOTES

12a. DISTRIBUTION / AVAILABILITY STATEMENT

Approved for public release; distribution unlimited.

12b. DISTRIBUTION CODE

13. ABSTRACT *(Maximum 200 words)*

A review of fundamental shock-transition theory is presented. The equation of state (EOS) is introduced as an analytical vehicle to express material pressure as a function of density and temperature (or internal energy in the case of adiabatic transition).

Starting from the fundamental laws of thermodynamics, three criteria are developed to measure the stability of equations of state and are applied specifically to the Mie-Grüneisen EOS, with Hugoniot reference, to investigate the stability characteristics thereof. This EOS is singled out for study because of its relative importance in the computational modeling of shock transition. Results indicate numerous possibilities of instability under various circumstances. Various remedies are proposed to correct the observed instabilities and compared with existing models.

14. SUBJECT TERMS	15. NUMBER OF PAGES
Stability, Hugoniot, Shock, Equation of State, Shock Loading, Hydrocode	48
	16. PRICE CODE

17. SECURITY CLASSIFICATION OF REPORT	18. SECURITY CLASSIFICATION OF THIS PAGE	19. SECURITY CLASSIFICATION OF ABSTRACT	20. LIMITATION OF ABSTRACT
UNCLASSIFIED	UNCLASSIFIED	UNCLASSIFIED	UL

INTENTIONALLY LEFT BLANK.

TABLE OF CONTENTS

LIST OF FIGURES

LIST OF TABLES

INTENTIONALLY LEFT BLANK.

1. INTRODUCTION

With the widespread use of numerical (hydro-) codes to describe the behavior of bodies impacting at high velocity, it is vital that code developers and users be familiar with the various numerical models in the codes. All too often, effort is concentrated on the "numerics" of a code, such as integration and discretization techniques, artificial viscosity formulations, mass lumping and pressure averaging techniques, and mass advection schemes, with the same rigor being absent when considering the "physics" of the code.

Because code development involves significant effort, it is common for codes to evolve or be passed down directly, rather than be written from the ground up. With this sort of evolution, it is possible to avoid "reinventing the wheel." Unfortunately, this mentality, if taken to the extreme, precludes the ability to redesign the "wheel" and can result in an incompatible combination of "wheel" and code "vehicle." Common problems associated with material model evolution are enumerated below:

(1) Many material models are based on assumptions and limitations which are often not passed on with the model. Thus, material models which are valid only for a particular class of problems (e.g., small compression, ductile behavior, etc.) can be erroneously applied to more general classes of problems.

(2) Goodness of a material model is often judged on its ability to solve a particular set of problems, rather than on adherance to fundamental principles. Such heuristic approaches (e.g., use of non-associated flow rules) can be exercised with caution but often become institutionalized and taken as fact by an unknowing community.

(3) Many new material models are derived by applying ad hoc modifications to older models, rather than rederiving the models from basic principles. When this is done carelessly, conflicting assumptions or limitations can render such models invalid.

(4) Material libraries tend to take on a life of their own and are passed down from generation to generation without the accompanying experimental data used to generate those libraries.

When this happens, material data are often used under conditions (e.g., strain rates, pressures, etc.) where those data are not valid.

One aspect of material modeling which is extremely important to impact codes, and to which all of the abovementioned problems are relevant, is the equation of state (EOS). In this report, equations of state for use in impact codes are discussed in general terms, with the Mie-Grüneisen equation of state used for specific illustrative purposes since it is the workhorse EOS of the current generation of hydrodynamic wave codes. Basic derivations, assumptions, and limitations of applicability are all discussed, with the prime focus being on equation-of-state stability.

2. THERMODYNAMIC STATES AND THE EQUATION OF STATE

To completely describe the volumetric behavior of a material, the values of the thermodynamic state variables (i.e., the thermodynamic coordinates) are needed for every state of the material. Thermodynamic state variables are properties which are only dependent on the state of a material and not on the path taken to arrive at that state. Examples of typical thermodynamic state variables include pressure and temperature, as well as specific volume, internal energy, enthalpy, entropy, etc.

To describe the state of a simple substance, excluding such phenomena as phase change, dissociation, or electromagnetic work, a knowledge of the material's pressure, as a function of density and temperature, is sufficient to completely describe the state of a material. In general, these thermodynamic state data are related in one of three forms.

Tabulated experimental data is one popular form of representing thermodynamic state data. Steam tables are probably the most widely used form of tabulated thermodynamic data. Data are tabulated over a large range of states, and interpolation becomes necessary to obtain data between the tabulated state points.

Of a similar nature to tabulated thermodynamic data is graphical thermodynamic data. The Mollier diagram, which graphically represents the states of water in its various phases, is the classic example of graphically represented thermodynamic data. To the experienced user, graphical state tables provide a fast, accurate means of evaluating the change in state variables, when something is

known about the thermodynamic process in question. Like tabulated data, extensive experimental testing is necessary to generate the data found in graphical thermodynamic state tables.

The third, and possibly most common, way to represent thermodynamic state data is in analytical form, and is referred to as an equation of state. Traditionally, the EOS expresses pressure in terms of density and temperature. Describing material by way of an EOS has many advantages. The form is compact, much more so than exhaustive tabulated data. An EOS may be mathematically codified, thus making it the most attractive on the basis of programming considerations. Additionally, the interrelationship of state variables may be mathematically derived from the EOS, thus providing a more fundamental understanding of the thermodynamic phenomena at work.

On the other hand, equations of state can suffer from severe deficiencies, which can make their use prone to error. Invariably, equations of state are formulated, with a host of inherent assumptions about the nature of the material behavior. Common examples of such assumptions include constant specific heats, ideal gas, etc. While these assumptions may be valid over a small domain of possible states, they are often poor at describing the material under extreme thermodynamic conditions like high/low pressure, phase change, and the like. This limitation, in and of itself, is not bad. However, those who use these equations are not always cognizant of the conditions under which a given EOS is valid. Thus, equations of state may be used in a thermodynamic domain where the EOS parameters are no longer valid. Also, there can be a problem with EOS forms which, though capturing the essence of the material behavior, suffer from "higher order" inconsistencies that only manifest themselves obliquely.

When it comes to hydrocode modeling of material deformation, where the EOS is just a means to a computational end, sophistocated equations of state, though available in the literature, are rarely used because of simplicity (i.e., efficiency) considerations. This focus on computational simplicity merely serves to enhance the likelihood of EOS failure in hydrocode computations.

All equations of state need data with which to drive themselves. In the case of the Mie-Grüneisen EOS, as used in today's hydrocodes, thermodynamic state variables are expressed relative to those states found along an experimentally determined pressure-volume curve which, for the case of impact data, is usually chosen as the Hugoniot curve. Thus, before the Mie-Grüneisen EOS can be discussed

in detail, the reader must acquire an appreciation of the Hugoniot and the thermodynamic process of shock transition.

3. SHOCK TRANSITION: A THERMODYNAMIC PROCESS

A shock is a volumetric disturbance which travels faster, in a medium, than the bulk speed of sound (i.e., sonic velocity) characteristic to the state of that medium. A shock is characterized by a shock front, which itself is very thin (thickness on the order of micrometers), and is analytically idealized as a discontinuity in physical properties such as density, pressure, and energy. The thinness of the shock coupled with the high velocity of the shock front ensure the adiabatic nature of shock transition. Large amplitude disturbances are not necessarily shocks if the thickness of the disturbance is relatively large. Correspondingly, the amplitude of a shock need not be necessarily large as long as the disturbance is traveling faster than the sonic velocity.

Shock transition may be thought of as an adiabatic irreversible thermodynamic process which permits the state of a material to be altered in a fashion similar to isentropic, isothermal, isochoric, isenthalpic, and isobaric processes. Whereas all of these other thermodynamic processes are characterized by the constancy of a particular state variable, the process of shock transition is characterized only by the existence of a shock wave. No thermodynamic state variables remain constant during shock transition. Nonetheless, the shock transition process can be as well characterized as any of the other thermodynamic processes, as will be shown from the following derivation of the basic shock relations.

4. BASIC SHOCK EQUATIONS

Consider a shock disturbance traveling at velocity U_s into a stationary medium, with density, pressure, and specific internal energy of ρ_o, p_o, and E_o, respectively. Behind the shock, the material has acquired a particle velocity, given by u_p, traveling in the same direction as the shock disturbance. The density, pressure, and specific internal energy are ρ, p, and E, respectively. This situation is depicted in the Laboratory Frame diagram of Figure 1. If an observer could be situated right on the shock wave, so that the shock were to appear stationary, the situation would appear like that depicted

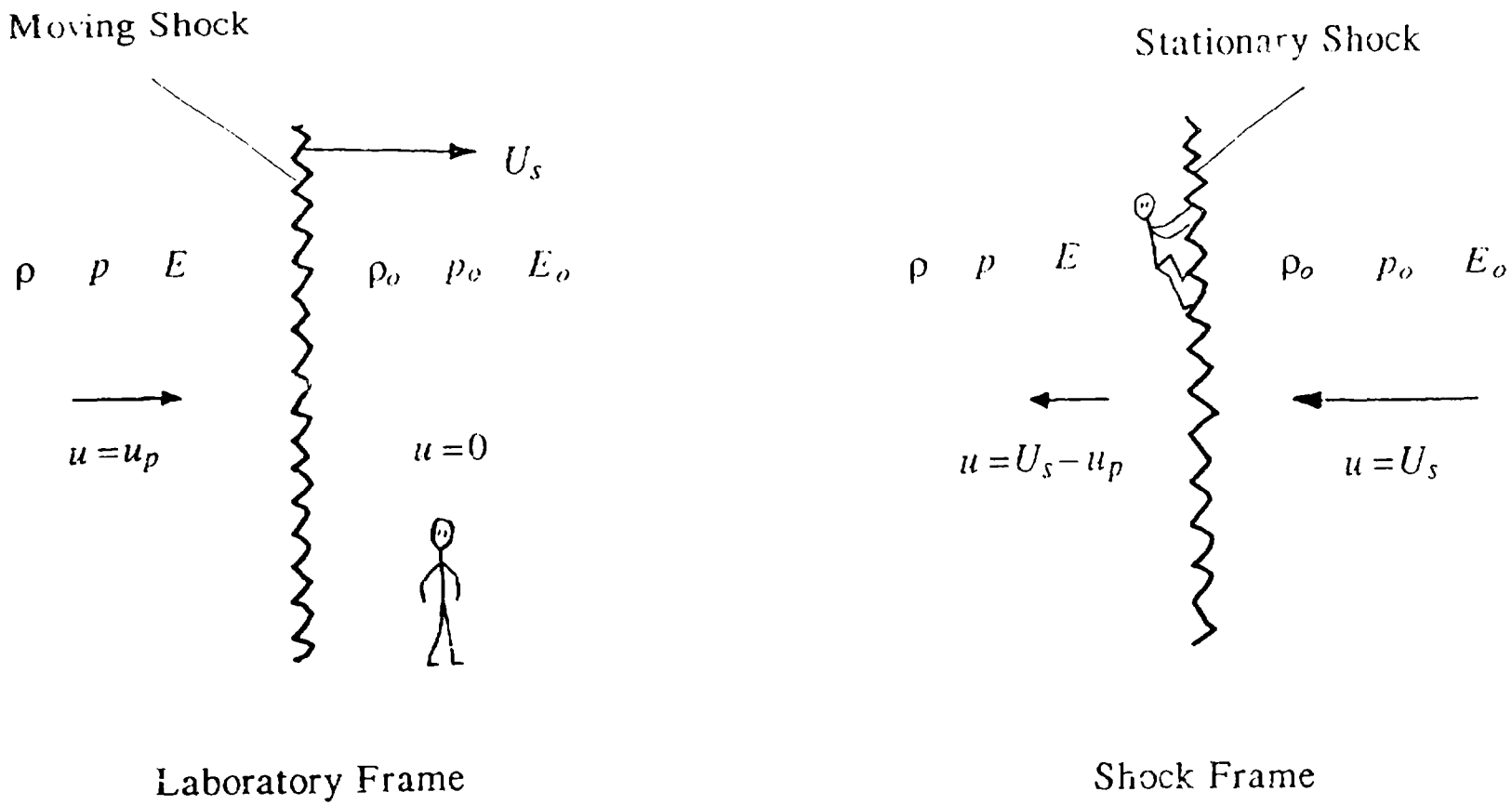

Figure 1. Depiction of Laboratory and Shock Reference Frames, Used to Derive Continuity, Momentum, and Energy Relations for Shock Transition (Zucker 1977).

in the Stationary Shock Frame diagram. The continuity, momentum, and energy relations are derived below by considering an infinitesimally thin contol volume, which fluxes mass dM, over a time increment dt, which straddles the shock front, in the stationary shock frame. The control volume projects unit area A onto the shock front.

CONTINUITY:

Mass In : $\rho_o U_s A\, dt$

Mass Out: $\rho\,(U_s - u_p)\, A\, dt$

$$\frac{\rho}{\rho_o} = \frac{U_s}{U_s - u_p}$$

Or, in terms of compression μ:

$$\mu = \frac{u_p}{U_s - u_p}\ ; \quad \text{where } \mu = \frac{\rho}{\rho_o} - 1$$

MOMENTUM:

Decelerative Impulse: $(p - p_o)\, A\, dt$

Momentum Decrease: $dM\,[U_s - (U_s - u_p)] = (\rho_o U_s A\, dt)\,[U_s - (U_s - u_p)]$

$$p - p_o = \rho_o U_s u_p; \quad \text{for } p_o \approx 0, \quad p = \rho_o U_s u_p$$

ENERGY:

Energy In:

Internal Energy In : $E_o\, dM = E_o\,(\rho_o U_s A\, dt)$

Kinetic Energy In : $1/2\, dM\, U_s^2 = 1/2\,(\rho_o U_s A\, dt)\, U_s^2$

Net Work on Control Volume: $\Sigma F\, dx = (p_o A)\,(U_s\, dt) - (p A)\,[(U_s - u_p)\, dt]$

Energy Out:

Internal Energy Out : $E\ dM = E\ (\rho_o U_s A\, dt)$

Kinetic Energy Out : $1/2\ dM\ u_p^2 = 1/2\ (\rho_o\ U_s\ A\ dt)\ (U_s - u_p)^2$

Internal Energy Accumulated: 0

$$E - E_o = 1/2\ (p + p_o)(1/\rho_o - 1/\rho);\quad for\ p_o \approx 0,\quad E - E_o = 1/2\ p(1/\rho_o - 1/\rho)$$

Or, in terms of compression μ:

$$E - E_o = \frac{(p + p_o)\ \mu}{2\rho_o\ (1 + \mu)};\quad \text{for } p_o \approx 0,\quad E - E_o = \frac{p\ \mu}{2\rho_o\ (1 + \mu)}$$

5. THE HUGONIOT

The momentum relation derived above expresses pressure in terms of shock and particle velocities, U_s and u_p, respectively. If the nature of the shock or particle velocity relationships are explicitly known, then the pressure can be expressed in terms of specific volume v, density ρ, or alternately, compression μ. This pressure-volume relationship for the shock compression process is called the Rankine-Hugoniot equation—or more simply, the Hugoniot—and is the locus of states which can be achieved through the shock transition of a material from a given (p_o, v_o) state.

It is vital to note that the Hugoniot does not represent the actual path of states through which a material progresses, when transitioning from the (p_o, v_o) state to (p, v), but rather the locus of final (p, v) states which can be achieved through shock transition. Also, since we know shock transition to be a compressive proccess only, a particular Hugoniot curve has one endpoint: the pre-shocked (p_o, v_o) state. From this endpoint, the Hugoniot proceeds in the direction of increasing pressure and decreasing volume.

Examining the shock energy relationship for the case of an infinitesimal shock, it is seen that $dE = -p_o\ dv$, which exactly equals the reversible work that is done on the material during the infinitesimal compression. This condition makes the process reversible adiabatic, thus isentropic. The implication is that at its endpoint, the Hugoniot is tangent to the isentrope through that point. Except

at its endpoint however, the Hugoniot slope (with respect to density) is necessarily steeper than the isentrope through a given point.

Unlike other thermodynamic processes, for example isentropic compression, where knowledge of a single state on an isentropic (p, v) curve is sufficient to completely describe that isentropic curve, knowledge of a state point on a Hugoniot curve is not sufficient to define the Hugoniot curve. That is to say, there are many (p_o, v_o) states which can possibly shock transition to state (p, v). This is identical to saying that there are many Hugoniots through any state point, as we shall prove in the next section.

6. SOME PROPERTIES OF THE HUGONIOT

To prove the assertion that there is no unique Hugoniot through the state point (p, v), let us assume the contrary and show an inconsistency. Consider the Hugoniot referenced to state (p_o, v_o) (we will hereafter call this the (p_o, v_o) Hugoniot) which goes through state point (p, v). Consider also another Hugoniot, referenced to state (p_1, v_1), which also goes through state (p, v). If one assumes that there is a unique Hugoniot which goes through the state (p, v), then one is forced to conclude that both states (p_o, v_o) and (p_1, v_1) lie along this unique Hugoniot. If (p_1, v_1) is in fact on the (p_o, v_o) Hugoniot, then shock transition can theoretically occur from the state (p_o, v_o) to (p_1, v_1).

To show the inconsistency which arises from this assumption, consider the changes in specific internal energies which arise when shock transitioning from states (p_o, v_o) to (p, v), from (p_1, v_1) to (p, v) and also from (p_o, v_o) to (p_1, v_1).

$$E - E_o = 1/2\ (p_o + p)\ (v_o - v)\ ,$$

$$E - E_1 = 1/2\ (p_1 + p)\ (v_1 - v)\ ,$$

$$E_1 - E_o = 1/2\ (p_o + p_1)\ (v_o - v_1)\ .$$

Subtracting the second two equations from the first should produce an identity, but it can be readily seen that not all of the terms cancel:

$$0 = 1/2 \left[p_o (v_1 - v) + p (v_o - v_1) - p_1 (v_o - v) \right] .$$

This can be reduced to:

$$(p_1 - p_o) / (v_o - v_1) = (p - p_1) / (v_1 - v) .$$

Not only is this expression not an identity, but it will only reduce to a true statement if the Hugoniot coincides with a Rayleigh line, which is line of constant slope in the (p, v) plane. Additionally, thermodynamics tells us that there exists a local maxima of entropy along a Rayleigh line, where it is tangent to an isentrope. Thus, the Hugoniot cannot possibly lie along a Rayleigh line, for to do so would imply decreasing entropy with increasing shock strength as the shocked state moved beyond the local entropy maxima on the Rayleigh line.

Thus, the inconsistency has been shown, and one can conclude that the assumption that both (p_o, v_o) and (p_1, v_1) lie on the same unique Hugoniot must be false, even though the Hugoniots originating at both these points intersect at the point (p, v).

A corollary to this point is that, if one were to proceed from state (p_o, v_o) towards a specific volume of v, by way of two shocks, the final pressure will not be the same as when specific volume v is achieved through a single shock, since the new Hugoniot originating at the intermediate shocked state will differ from original (p_o, v_o) Hugoniot. In the limit, if the specific volume v is reached through an infinite number of infinitesimal shocks, it should not be surprising that the path of compression will lie along the isentrope through the original (p_o, v_o) point, since an infinitesimal shock was shown previously to be isentropic.

In practice, only a single Hugoniot is experimentally determined to characterize the behavior of a material—that Hugoniot which has as its (p_o, v_o) state ambient conditions of pressure and specific volume. Thus, references to "the" Hugoniot for a material refer to a particular "reference" Hugoniot which has as its origin the ambient (p_o, v_o) state.

7. EXAMINATION OF SEVERAL HUGONIOT FORMS

7.1 Constant Sound Speed. Constant sound speed implies that all disturbances travel at the same velocity, or

$$U_s = C_o .$$

Determining the particle velocity from continuity gives

$$u_p = C_o (1 - \rho_o/\rho) .$$

It is clear that the particle velocity can never exceed the shock velocity and simultaneously satisfy continuity, so the implication is that the maximum possible particle velocity is also the shock velocity C_o, and this only occurs as the shocked density becomes infinite. It should be clear from momentum considerations, therefore, that the maximum pressure achievable in a constant sound speed medium is $\rho_o C_o^2$. Indeed, the relation is given by

$$p_h - p_o = \frac{\rho_o C_o^2 \mu}{(1 + \mu)} .$$

7.2 The Ideal Gas Form. Much of the work done in thermodynamics is done on the assumption that the working medium may be approximated as an ideal gas. Unfortunately, at large compressions, materials do not generally behave in an ideal fashion. Nonetheless, we examine the Hugoniot form for the sake of academic interest.

An ideal gas is one which obeys the EOS $p/\rho = RT$, where R is the gas constant, and T is the gas temperature. Additionally, an ideal gas is assumed to have constant specific heats c_p and c_v. Under these conditons of idealness, $E = c_v T$, and the EOS may be expressed as $p/\rho = (R/c_v) E$. But $R = c_p - c_v$ by definition, and the ratio c_p/c_v is often expressed as γ, so that

$$p = \rho (\gamma - 1) E .$$

Consider the shock energy equation, and eliminate energy terms from it by substituting the gamma law from above. In that case,

$$\frac{p_h}{\rho (\gamma - 1)} - \frac{p_o}{\rho_o (\gamma - 1)} = (p_o + p_h) (1/\rho_o - 1/\rho) .$$

This may be solved for the Hugoniot pressure p_h, and expressed in compression form, by substituting $(1 + \mu)$ for ρ/ρ_o, to give

$$p_h/p_o = \frac{(\gamma + 1)(1 + \mu) - (\gamma - 1)}{(\gamma + 1) - (\gamma - 1)(1 + \mu)} .$$

Expressed in a $(p_h - p_o)$ form, it becomes

$$p_h - p_o = \frac{2\gamma\mu}{2 - (\gamma - 1)\mu} .$$

This Hugoniot form is seen to approach infinite pressure when

$$\mu = 2/(\gamma - 1) .$$

This limit, expressed in terms of density, is

$$\rho/\rho_o = \frac{\gamma + 1}{\gamma - 1} .$$

7.3 The Linear U_s - u_p Form. It has been empirically observed for many materials, over a significant range of pressures, that the relationship between the shock and particle velocity can often be fit by a straight line, as in

$$U_s = C_o + S\,u_p .$$

Thus,

$$p_h - p_o = \rho_o\,(C_o + S\,u_p)\,u_p ,$$

and from continuity, particle velocity may be determined as

$$u_p = \frac{\eta C_o}{1 - \eta S} \text{ , where } \eta = 1 - \rho_o/\rho \text{ .}$$

Particle velocity may be eliminated from these equations to give

$$p_h - p_o = \frac{\rho_o C_o^2 \eta}{(1 - \eta S)^2} \text{ .}$$

Expressing this in compression form gives:

$$p_h - p_o = \frac{\rho_o C_o^2 \mu (1 + \mu)}{(1 - (S - 1)\mu)^2} \text{ .}$$

It can be seen, for S > 1, that this linear U_s - u_p Hugoniot equation approaches infinite pressure at finite compression ($\mu = 1/[S - 1]$), not unlike the ideal gas EOS. Otherwise, for S < 1, the Hugoniot pressure converges to $\rho_o C_o^2/(S - 1)^2$ for large μ. Also, the special case of S = 0 reduces to the previously derived situation of constant sound speed. This finite limiting pressure for S < 1 arises because the U_s function intersects the u_p function at $U_s = C_o/(1 - S)$. Since U_s must always exceed u_p, these limiting values of U_s and u_p cause the limiting value in pressure too. Though this $U_s = u_p$ condition is unrealistic, apparently several materials exhibit S < 1 at lower compressions (Kohn 1969). Such data can be misleading, and can cause problems if S < 1 is retained out to larger compressions in numerical simulations.

7.4 The Polynomial Hugoniot. Often, a form is not assumed on the U_s - u_p relation, or the compressibility at all, but rather, an empirical fit is made directly to the Hugoniot, as in

$$p_h - p_o = \sum_{i=1}^{n} K_i \mu^i \text{ ,}$$

where K_i are the empirical constants, and n is the order of the polynomial fit. A popular value for n is three, giving a cubic fit. Note the functionally different forms between this Hugoniot form and the linear U_s - u_p form, for instance. To work the problem in reverse, and obtain the shock velocity for a cubic Hugoniot fit, for example, one can manipulate continuity and momentum equations to get:

$$U_s^2 = [K_1 + (K_1 + K_2)\,\mu + (K_2 + K_3)\,\mu^2 + K_3\mu^3] / \rho_o .$$

Note that U_s^2 at $\mu = 0$, which is C_o^2, equals K_1/ρ_o.

8. THE IMPORTANCE OF DISTURBANCE VELOCITY ON NUMERICAL STABILITY

The primary emphasis in describing the shock loading behavior of materials has been on the Hugoniot fit itself, the p_h vs. μ relation. However, the importance of the disturbance speeds U_s and C (i.e., the shock velocity and local sound speed) cannot be underestimated. In impact computations, where the wave motions are the important part of the problem solution, knowledge of disturbance velocities becomes necessary for accuracy, and in explicit schemes, for stability, of the calculation.

In explicit integration schemes, which are by far the most prevalent in use for impact calculations, stability requirements place limitations on the integration timestep. In particular, the explicit integration timestep must be limited so that a disturbance can traverse no more than a single computational zone per integration cycle. To enforce this requirement, one needs knowledge of both the particular zone size in question and the disturbance velocity in that computational zone. The former is simply a function of zone geometry, while the latter is the shock velocity U_s, when the material is compressing, and the sound speed C, when the material is expanding. Thus, an accurate knowledge of disturbance velocities U_s and C, under various states of loading, is vital to the numerical stability of explicit integration schemes.

In addition to the effect of the disturbance velocities on the stability of the explicit numerical integration scheme, these velocities are intimately related to the stability of the EOS calculation itself, even in the absence of a numerical code application. There are thermodynamic considerations which must be satisfied by any valid EOS.

Three particular modes of EOS instability will be addressed in the following sections. Stated in English, these stability criteria sound almost trivial, since they immediately result from fundamental thermodynamic statements, which have been known and professed for years. Nonetheless, these

criteria, which can be expressed mathematically, and are tested in the framework of the Mie-Grüneisen EOS, show a necessary interrelation amongst various EOS parameters, which is not commonly appreciated. As such, indiscriminate choice of parameters to drive the EOS will often cause at least one of these criteria to be violated. Use of such data in a numerical scheme can result in bizzarre manifestations of numerical instability.

The three stability criteria are given below and apply to materials where phase changes and/or porosity are not considered (i.e., simple substances). For the first two criteria, consider a state (p, v), which lies on the Hugoniot originating from the state (p_o, v_o).

(I) at the state (p, v), the slope of the Hugoniot with respect to density must exceed the slope of the Rayleigh line connecting states (p_o, v_o) and (p, v);

(II) at the state (p, v), the slope of the isentrope must lie between the slope of the Hugoniot, and the slope of the Rayleigh line connecting states (p_o, v_o) and (p, v);

(III) the slope of an isentrope with respect to density is always greater than zero.

From the second law of thermodynamics, it is known that entropy is monotonically increasing along a Hugoniot. By definition, entropy is constant along an isentrope. Finally, a Rayleigh line is known to have one point of maximum entropy. It can be shown (Zuker 1977) that this point of maximum entropy lies between the states (p_o, v_o) and (p, v). Thus, at the state (p, v) and traveling in the direction of increasing density, entropy must be decreasing. Criteria I and II express this relational placement of the Rayleigh line, the isentrope and the Hugoniot. Criterion III simply implies the obvious, that the speed of sound in a material is a positive quantity.

9. MODE I INSTABILITY OF SEVERAL HUGONIOT FORMS

It was mentioned that a Hugoniot has the slope (with respect to density ρ or compression μ) of the isentrope only at the end point of the Hugoniot. At other points along the Hugoniot, the Hugoniot will always be steeper than the corresponding isentrope. Let us examine the two most popular Hugoniot forms (linear U_s - u_p fit and cubic fit) to check their adherence to these rules. The slope of the

Hugoniot at any point on the Hugoniot is simply $dp_h/d\rho$. Total derivatives are used since, along the Hugoniot, pressure is only a function of a single variable (ρ, μ, or v, at the discretion of the user). To determine the slope of the isentrope at that point, one can make use of the definition that $\partial p/\partial \rho \,|_s$ equals the square of the sonic velocity.

For the case of the linear U_s - u_p fit, recall that

$$p_h - p_o = \frac{\rho_o C_o^2 \mu (1 + \mu)}{(1 - (S - 1)\mu)^2} .$$

Taking the derivative with respect to μ, one may obtain

$$\frac{dp_h}{d\mu} = \frac{\rho_o C_o^2 [1 + (S + 1)\mu]}{[1 - (S - 1)\mu]^3} .$$

The chain rule dictates that $dp_h/d\rho = dp_h/d\mu \; d\mu/d\rho$, where $d\mu/d\rho$ is simply $1/\rho_o$, so that

$$\frac{dp_h}{d\rho} = \frac{C_o^2 [1 + (S + 1)\mu]}{[1 - (S - 1)\mu]^3} .$$

Without knowing additional information about the EOS, the slope of the post shock isentrope $\partial p/\partial \rho \,|_s = C^2$, and, thus, the sonic velocity C, cannot be explicitly determined after a shock. However, the particle velocity relative to the stationary shock front after a shock, equal to $(U_s - u_p)$, is known to be subsonic. It may also be shown that $\partial p/\partial \rho$ along the Rayleigh line connecting the pre- and post-shocked states exactly equals $(U_s - u_p)^2$. If the Hugoniot slope is larger than the slope of the actual isentrope, then clearly its slope must be larger than that of the Rayleigh line, which represents the lower bound on the slope of the isentrope.

From continuity, the quantity $(U_s - u_p)$ may be expressed either as $U_s/(1 + \mu)$ or u_p/μ. Thus, the slope of the isentrope $\partial p/\partial \rho \,|_s = C^2$ must be greater than $U_s^2/(1 + \mu)^2$, which is the slope of the Rayleigh line. Now, consider the Rayleigh line slope at some point on the Hugoniot. For the linear U_s - u_p assumption, $U_s = C_o + S\, u_p$. However, it is desired to obtain U_s in terms of compression μ.

Elimination of u_p from the continuity equation gives,

$$\mu = \frac{u_p}{U_s - u_p} = \frac{(U_s - C_o)/S}{U_s - (U_s - C_o)/S} .$$

Upon solution for U_s,

$$U_s = \frac{C_o(1 + \mu)}{[1 - (S - 1)\mu]} .$$

Thus, $\partial p/\partial \rho \,|_R = U_s^2/(1 + \mu)^2$, and is given as

$$\left.\frac{\partial p}{\partial \rho}\right|_R = \frac{C_o^2}{[1 - (S - 1)\mu]^2} .$$

For the Hugoniot slope to exceed the corresponding Rayleigh line slope for all $\mu > 0$, the ratio of $dp_h/d\rho$ to $\partial p/\partial \rho \,|_R$ must always exceed unity. Failure to do so implies that there can exist no valid equation of state to describe the material. We will call Hugoniots whose slope does not exceed that of the corresponding Rayleigh line, as Mode I unstable. Mathematically, the condition is stated below:

MODE I CRITERION:

$$\frac{dp_h/d\rho}{\partial p/\partial \rho|_R} > 1 , \text{ for } \mu > 0, \text{ along the Hugoniot.}$$

For the linear U_s - u_p form, the stability ratio, which must exceed unity, is given by

$$\frac{dp_h/d\rho}{\partial p/\partial \rho|_R} = \frac{[1 + (S + 1)\mu]}{[1 - (S - 1)\mu]} > 1 , \text{ for } \mu > 0, \text{ along the Hugoniot.}$$

Clearly, for any S greater than zero, the stability criterion is not violated. Thus, the linear U_s - u_p formulation is always Mode I stable.

Considering now the cubic empirical Hugoniot fit, it is of interest to see how this Hugoniot form fares with the Mode I stability criterion. Mimicking the operations performed on the U_s - u_p forms, $dp_h/d\rho$ is determined as

$$\frac{dp_h}{d\rho} = \left[K_1 + 2K_2\,\mu + 3K_3\,\mu^2\right]/\,\rho_o \,.$$

The slope of the Rayleigh line, $\partial p/\partial \rho\,|_R$ equals $U_s^2/(1+\mu)^2$, and is given by

$$\left.\frac{\partial p}{\partial \rho}\right|_R = \frac{K_1 + (K_1 + K_2)\,\mu + (K_2 + K_3)\,\mu^2 + K_3\,\mu^3}{\rho_o\,(1+\mu)^2} \,.$$

Finally, the Mode I stability criterion, which insures that the slope of the Hugoniot exceeds that of the Rayleigh line connecting the pre- and post-shocked states, is given as

$$\frac{dp_h/d\rho}{\partial p/\partial \rho\,|_R} = \frac{\left(K_1 + 2K_2\,\mu + 3K_3\,\mu^2\right)(1+\mu)^2}{K_1 + (K_1 + K_2)\,\mu + (K_2 + K_3)\,\mu^2 + K_3\,\mu^3} > 1 \,,$$

for $\mu > 0$, along the Hugoniot. Because of the dependence of this term on three independent parameters, a simple answer cannot be given. However, the data collected and fit by Kohn (1969) into K_1, K_2, K_3 form can still be checked for slope violations. It was found that 21 of 77, or 27%, of the materials violated the criterion in part of the compression range where the empirical fit was supposedly valid. Perhaps this behavior can be attributed to the forcing of a cubic Hugoniot function onto a highly non-linear material response, possibly due to phase changes. In such cases, Mode I instability implies that a cubic Hugoniot fit is inadequate. The ramifications of Mode I instability on computational stability are not as clear as the other modes to be discussed, where instability is more likely to guarantee computational catastrophe.

10. INTRODUCTION TO THE MIE-GRÜNEISEN EQUATION OF STATE

Traditionally, an EOS is an equation which describes the pressure of a material as a function of density and temperature. It is needed to solve the continuity, momentum, and energy equations which govern the thermodynamic transition of a material. In the case of impact though, thermodynamic

states change so rapidly that there is little time for heat transfer. Under these conditions of adiabatic transition, the energy equation need not explicitly contain temperature, and the governing equations may be solved if either the entropy or the internal energy is known as a function of pressure and density (Zeldovich and Razier 1966). The Mie-Grüneisen EOS is of this variety, in that internal energy, and not temperature, is related to pressure and density. The penalty for not having the traditional p (ρ, T) formulation is that temperature is not a computable state variable.

For impact calculations, accurate description of shock transition states is very important. Additionally, high pressure material data are usually obtained from shock transition experiments and is given in the form of a Hugoniot curve. The Hugoniot provides the means to ascertain the pressure and internal energy as a function of compression for those thermodynamic states which can be achieved through shock compression of a material.

Thus, realizing that an EOS is only an approximation to the actual behavior of a material, it seems desirable to have an EOS which is very accurate along the path where data are available (i.e., along the experimentally derived Hugoniot). State points other than those found directly on the Hugoniot are obtained from an EOS which references material back to the state along this reference Hugoniot. The Mie-Grüneisen EOS provides the framework through which state points can be tied back to an arbitrary reference function, as described below.

Consider the textbook form of the Mie-Grüneisen EOS (McQuarrie 1976), expressed in terms of density

$$p = \rho^2 \frac{dU}{d\rho} + \Gamma \rho (E - U) ,$$

where U is the specific interatomic potential energy (a function of density only), and E is the specific internal energy comprised of both interatomic potential (i.e., compressive) energy and atomic vibrational (i.e., thermal) energy. Note that the term ρ^2 dU/dρ represents the "cold pressure," which is that pressure arising from compression at absolute zero temperature, in the absence of specific vibrational internal energy (E-U). The term Γ is the Grüneisen coefficient, which is a function of density only, derived by assuming a particular form on the vibrational frequencies of the crystal lattice.

If the cold pressure curve is known (or assumed), and if the thermodynamic states are known along another reference curve (e.g., the Hugoniot), then the Grüneisen coefficient may be inferred

directly, as a function of density. On the other hand, if the thermodynamic states are known only along a "non-cold" reference curve, but if a functional relationship is assumed for the Grüneisen coefficient, then the interatomic potential function may be implicitly removed, by referencing the thermodynamic state at any point (p, ρ, E) back to the state along the reference curve, at the same density (p_{ref}, ρ, E_{ref}). This is done by taking the difference of the Mie-Grüneisen EOS, given above, at the two state points in question. It is this approach which is almost universally adopted by hydrocodes, to give

$$(p - p_{ref}) = \Gamma \rho (E - E_{ref}) .$$

It should be noted that the interatomic potential, U, and thus the cold pressure curve, may be recovered, by solving the following non-linear ordinary differential equation:

$$\frac{dU}{d\rho} - \frac{\Gamma U}{\rho} = \frac{\phi(\rho)}{\rho^2} ,$$

where $\phi(\rho)$ is a function of density only, obtained from the "non-cold" reference curve and the assumed Grüneisen function:

$$\phi(\rho) = p_{ref} - \Gamma \rho E_{ref} .$$

For the present purposes, the reference function is chosen as the Hugoniot, so that the Mie-Grüneisen EOS becomes

$$(p - p_h) = \Gamma \rho (E - E_h) .$$

The quantities p_h and E_h are the pressure and specific internal energy of the reference Hugoniot state point at the same density as the state (p, ρ, E) in question. Often, the shock energy equation is substituted directly into the Mie-Grüneisen EOS to give

$$p = p_h(1 - \Gamma\mu/2) + \rho_o\Gamma (1 + \mu) [E - E_o] - p_o\Gamma\mu/2 .$$

The ambient conditions p_o, E_o, are generally pegged at zero, so that the Mie-Grüneisen EOS, with Hugoniot reference, is expressed as

$$p = p_h (1 - \Gamma\mu/2) + \rho_o\Gamma (1 + \mu) E .$$

Note, in an analogous fashion to the Mie-Grüneisen EOS, that ideal gas behavior may be modeled if $\frac{1}{\rho}\left.\frac{\partial p}{\partial E}\right|_{\rho}$, given by Γ for solids, is held constant for gases, equal to $(\gamma - 1)$, and if the Hugoniot form is that for an ideal gas; namely,

$$p_h - p_o = \frac{2\gamma\mu}{2 - (\gamma - 1)\mu} .$$

The Mie-Grüneisen EOS, with Hugoniot reference, is only valid where the Hugoniot reference is valid. If the reference Hugoniot is obtained by shocking material from ambient conditions, then clearly the Hugoniot is only valid in some region $\mu > 0$. Hydrocode implementors often fail to deal with this fact accurately. It is well known that the Hugoniot curve is a very close approximation to the isentrope at small values of compression, and so the pressure reference function usually employed by hydrocodes in tension is the isentrope, which is generally approximated by a curve which matches value and slope of the Hugoniot at $\mu = 0$. There is nothing wrong with this assumption, but innaccuracies are introduced when the shock energy equation is still employed directly to compute the energy reference function, as in EPIC (Johnson, Colby, and Vavrick 1978), which is tantamount to assuming the existence of a tensile shock.

Clearly, the energy reference function to drive the Mie-Grüneisen EOS in tension should not be the shock energy equation

$$E_h - E_o = \frac{p_{ref}\,\mu}{2\rho_o(1+\mu)} \quad (\text{where } p_o = 0) ,$$

but rather some physically plausible function—for instance, the isentropic expansion integral of work:

$$E_{ref} - E_o = \int_0^{\mu} p_{ref}\,\frac{d\mu}{\rho_o(1+\mu)^2} .$$

One possible approximation for the isentropic release function for $\mu < 0$ is to assume constant compressibility. In this case, where $p_o = E_o = 0$ is assumed for simplicity,

$$p_{ref} = K_o \mu \ , \quad \text{and}$$

$$E_{ref} = \int_0^{\mu} p_{ref} \frac{d\mu}{\rho_o (1+\mu)^2} = (K_o/\rho_o) \left[ln\,(1+\mu) - \mu/(1+\mu) \right] .$$

Comparing the internal energy from this reference function to that computed from the invalid application of the shock energy equation in the tensile region, given by

$$E_h = \frac{p_{ref}\,\mu}{2\,\rho_o(1+\mu)} = \frac{K_o\,\mu^2}{2\,\rho_o(1+\mu)} ,$$

one may observe that the difference in computed internal energies is significant, as shown in Table 1.

TABLE 1. Comparing Internal Energies Resulting From Constant Compressibility "Isentropic" and "Tensile Shock" Expansions

μ	V/V_o	$\rho_o E/K_o$ (isentropic)	$\rho_o E_h/K_o$ (tensile shock)	% Error
0.0	1.00	0.	0.	0.
-.2	1.25	0.027	0.025	-7.4
-.4	1.67	0.156	0.133	-14.7
-.6	2.50	0.584	0.450	-23.1
-.8	5.00	2.39	1.60	-33.1

Other reasonable choices of isentropic release pressure reference functions may also be used in the region $\mu < 0$. For example, let the reference sound speed for a material in tension ($\mu < 0$) be described with the following function:

$$C = C_o (1+\mu)^{\beta} .$$

For this particular sound speed reference function, the tangent bulk modulus may be computed as

$$K = K_o (1+\mu)^{(2\beta+1)} .$$

This function has many nice properties. Two such advantages are that it reduces to constant compressibility for g = -1/2, and to constant sound speed for g = 0. Additionally, the sonic velocity is at the proper value at $\mu = 0$ and, for g greater than zero, the sonic velocity drops off to zero when the material is infinitely expanded (at $\mu = -1$). Increasing the exponent g causes the sonic velocity to drop off more rapidly in tension and will limit the maximum value of tension achievable during an isentropic expansion, which is a material feature observed experimentally and often modeled computationally by way of a p_{min} parameter. The reference pressure function is acquired by integrating the tangent bulk modulus and is given below for g not equal to (-1/2):

$$p_{ref} = \int_0^{\mu} K \frac{d\mu}{(1+\mu)^2} = \frac{K_o}{(2g+2)} \left[(1+\mu)^{(2g+2)} - 1 \right] .$$

The reference energy function (for g not equal to -1/2) is acquired by integrating the reference pressure function:

$$E_{ref} = \int_0^{\mu} p_{ref} \frac{d\mu}{\rho_o (1+\mu)^2} = K_o \frac{\left[(1+\mu)^{(2g+2)} - 1 \right] - \mu (2g+2)}{\rho_o (2g+2)(2g+1)(1+\mu)} .$$

For the special case of constant sound speed adiabatic expansion from $\mu = 0$, the exponent g equals 0, and one gets:

$$p_{ref} = K_o (\mu + \mu^2)/2 \text{ , and}$$

$$E_{ref} = \frac{K_o \mu^2}{2 \rho_o (1+\mu)} .$$

On the other hand, the reference pressure may be limited to a tensile pressure of p_{min}, which occurs at infinite expansion, by defining the exponent g to be

$$g = \frac{K_o}{2 |p_{min}|} - 1 .$$

Using steel, as an example, where K_o = 1,380 kbar, and p_{min} = -35 kbar, g takes on a value in the vicinity of 19. For aluminum, where K_o = 700 kbar, and p_{min} = -10 kbar, the value g takes is approximately 34. Table 2 depicts the parameter relationships for g = 20.

TABLE 2. Values of Compression, Relative Volume, and Normalized Values of Sonic Velocity, Pressure, Tangent Bulk Modulus, and Secant Bulk Modulus, Respectively, for the Proposed Tension Limiting Model, With g = 20

μ	V/V_o	C/C_o	p_{ref}/p_{min}	K/K_o	$p/K_o\mu$
0.00	1.00	1.000	0.000	1.000	N/A
-.002	1.002	.961	.081	.921	.960
-.02	1.02	.668	.572	.437	.681
-.04	1.04	.442	.820	.188	.488
-.06	1.06	.290	.926	.079	.367
-.08	1.19	.189	.970	.033	.289
-.10	1.11	.122	.988	.013	.235

11. THE GRÜNEISEN PARAMETER

The Grüneisen parameter Γ is an important parameter used by the Mie-Grüneisen EOS. Though the assumption that Γ is a function of volume only is only an approximation, the parameter itself is not empirical but in fact carries physical significance. For ideal gases, the parameter analogous to Γ has been shown to be $(\gamma - 1)$. For solids, the parameter also has meaning.

To compute its value, consider a cube of material at state 1 characterized by pressure p and volume V. Let the material undergo a two-stage thermodynamic process. First, add heat dQ at constant pressure in order to go to state 2, characterized by p, V + dV. Finally, and with no heat addition, isentropically compress the material back to its original volume in order to arrive at state 3, characterized by p + dp, V.

During the process 1-2, the cube of material, the length of whose side was originally L, expands so that the length is now $L(1 + \alpha dT)$, where α is the coefficient of linear expansion. Thus, the relative volume change dV/V is given by $3\alpha dT$. The amount of heat added per unit mass dQ, is

$c_p\,dT$. For solids, which are nearly incompressible in comparison to gases, the specific heats at constant pressure and volume, c_p, and c_v, are nearly identical. Thus, the heat added can be approximated by $c_v\,dT$. The temperature change dT may be eliminated by relating dT back to volume change dV so that

$$dQ = \frac{c_v\,dV}{3\alpha V}.$$

The work done by the material per unit mass is negative since the volume change is the opposite sense of the pressure loads and is given by $dW = -p\,dV/(\rho V)$. From the first law of thermodynamics, the internal energy change dE, given by dQ - dW, can be expressed as

$$dE_{12} = \frac{c_v dV}{3\alpha V} + \frac{p\,dV}{\rho V}.$$

The process from state 2 to 3 has no heat addition, so dQ = 0. The work done by the system is $dW = (p + dp/2)\,dV/(\rho V)$ which, to the first order, is $p\,dV/(\rho V)$. The rise in internal energy is therefore the negative of the work

$$dE_{23} = \frac{p(-dV)}{\rho V}.$$

Thus, the difference between the pressures going from state 1 to 3 is dp, and the rise in internal energy is

$$dE_{13} = \frac{c_v dV}{3\alpha V}.$$

The volume of states 1 and 3 are identical, so that the Grüneisen parameter Γ will remain constant for the direct transition from state 1 to 3, when using the Mie-Grüneisen EOS, which relates states 1 and 3 as follows:

$$\frac{dp}{-(dV)} = \Gamma\rho\,\frac{c_v}{3\alpha V}.$$

But path 23 is isentropic, so that dp/(-dV) is $\partial p/\partial V\,|_s = (-\rho/V)\,\partial p/\partial \rho\,|_s$. But $\partial p/\partial \rho\,|_s$ is simply the square of the sound speed C, or alternately, the ratio of the bulk modulus and the density K/ρ. Substuting, and solving for Γ gives

$$\Gamma = \frac{3\alpha C^2}{c_v} = \frac{3\alpha K}{\rho c_v}.$$

From the Mie-Grüneisen EOS, it is clear that the Grüneisen parameter Γ relates changes in internal energy to changes in pressure at constant volume. As can be seen from the dimensional analysis of the second expression for Γ which follows, the numerator expresses the pressure rise per increment of temperature, while the denominator expresses the (volume-based) energy rise per increment of temperature. These terms combine in a way to produce a non-dimensional expression which represents the Grüneisen parameter.

$$\Gamma = \frac{3\alpha K}{\rho c_v} = \frac{\dfrac{dV/V}{deg}\,\dfrac{dp}{dV/V}}{\rho\,\dfrac{dE}{deg}} = \frac{dp/deg}{\rho\, dE/deg} = \frac{dp}{\rho\, dE} = [-].$$

Note: As in other places in this document, dE represents energy change per unit mass.

12. MODE II INSTABILITY OF THE MIE-GRÜNEISEN EQUATION OF STATE

Though there is nothing inherently wrong with the Mie-Grüneisen EOS, there are often situations where inappropriate choice of data forces a thermodynamic violation. As pointed out in the previous section dealing with Mode I instability, there are certain empirical Hugoniot fits which may violate fundamental thermodynamic rules. Clearly, plugging such fits into Mie-Grüneisen makes the possibility of catastrophic EOS failure significant. Additionally, there are inconsistent combinations of Hugoniot and Grüneisen functions which cause thermodynamic violations which are not immediately apparent.

To study these, consider a material in the state p_h, ρ, E_h on the Hugoniot originating at (p_o, v_o). From this state, consider two possible paths resulting from a small compressive increment, $d\rho$: the

path along the isentrope and also the path along the Hugoniot. Along the isentropic path, the pressure change is

$$\left.\frac{\partial p}{\partial \rho}\right|_s d\rho = C^2\, d\rho \ .$$

The internal energy change along the same path is the negative of the work, or

$$\left.\frac{\partial E}{\partial \rho}\right|_s d\rho = p_h\, (d\rho/\rho^2) \ .$$

Along the Hugoniot, the pressure change is simply $(dp_h/d\rho)\, d\rho$, and the energy change, may be obtained by taking the derivative of the shock energy relation $E_h - E_o = 1/2\ (p_h + p_o)\ (1/\rho_o - 1/\rho)$, to get

$$\frac{dE_h}{d\rho}\, d\rho = 1/2 \left[(p_h + p_o)/\rho^2 + (1/\rho_o - 1/\rho)\, dp_h/d\rho\right] d\rho \ .$$

If this material is to obey the Mie-Grüneisen EOS, then at the density $\rho + d\rho$,

$$\left[\left(p_h + \left.\frac{\partial p}{\partial \rho}\right|_s d\rho\right) - \left(p_h + \frac{dp_h}{d\rho}\, d\rho\right)\right] = \Gamma\, \rho \left[\left(E_h + \left.\frac{\partial E}{\partial \rho}\right|_s d\rho\right) - \left(E_h + \frac{dE_h}{d\rho}\, d\rho\right)\right] .$$

Canceling and substituting terms gives

$$(C^2 - dp_h/d\rho) = \Gamma\, \rho\, (p_h/\rho^2 - 1/2\ [(p_h + p_o)/\rho^2 + (1/\rho_o - 1/\rho)\, dp_h/d\rho]) \ .$$

Expressing this in terms of compression μ, and solving for Γ gives

$$\Gamma = \frac{2}{\mu}\, \frac{\left[\mu\, dp_h/d\mu - \mu\, \rho_o C^2\right]}{\left[\mu\, dp_h/d\mu - (p_h - p_o)/(1 + \mu)\right]} \ .$$

The significance of this expression is that, for a given Hugoniot relationship p_h as a function of μ, the Grüneisen coefficient Γ and the sound speed C are related. Since the sound speed is known to have thermodynamic limitations placed upon it, these limitations translate into constraints on the Grüneisen parameter Γ. Use of the Mie-Grüneisen EOS in codes, without the appropriate restraints on Γ, will usually result in catastrophic failure of the EOS.

To examine these constraints on Γ, consider the maximum and minimum possible values on C. Recall that the post shock particle velocity relative to the shock front, equal to $(U_s - u_p)$, is known to be subsonic, but approaches sonic conditions for infinitesimal shocks. Thus, as an absolute lower bound, let C approach $(U_s - u_p)$. This choice of C gives an upper bound on Γ. But $(U_s - u_p)$ equals $U_s/(1 + \mu)$, so that $(U_s - u_p)^2$ is given by

$$(U_s - u_p)^2 = U_s^2/(1 + \mu)^2 = (p_h - p_o)/[\rho_o \mu (1 + \mu)] .$$

Substituting this into the expression for Γ gives, as an upper bound,

$$\Gamma = 2/\mu .$$

For the lower bound on Γ, one may assume that the isentrope approaches the Hugoniot. In this case, $\partial p/d\mu \,|_s = dp_h/d\mu$. Since $\partial p/\partial \mu \,|_s$ equals $\rho_o C^2$ by definition, the minimum value on Γ may be determined as zero. By combining these two criteria, and calling them the Mode II stability criterion, one gets

MODE II CRITERION:

$$0 < \Gamma < (2/\mu) .$$

Failure to satisfy this criterion implies that the slope of the post shock isentrope does not fall between that of the Rayleigh line and the Hugoniot.

Recall, from the ideal gas form, that the parameter analogous to Γ is constant, and equal to $(\gamma - 1)$. It may at first appear that the ideal gas form violates the Mode II stability criterion for large μ. However, recall that infinite pressure was approached when the ideal gas compression μ equaled

$2/(\gamma - 1)$, which is $2/\Gamma$ in Mie-Grüneisen terms. Thus, over the physical μ domain of the ideal gas form, which is $\mu < 2/\Gamma$, Mode II stability is not violated.

In general though, it becomes clear that the terminal value of the Grüneisen coefficient, let us call it Γ_x, must be less than or equal to $2/\mu_x$, where μ_x is defined as that value of compression which produces infinite pressure in the Hugoniot. For the linear U_s - u_p form, μ_x occurs when the denominator $(1 - (S - 1)\,\mu)$ becomes zero, which occurs only if S exceeds unity. In this case,

$$\mu_x = 1/(S - 1) .$$

The value of Γ_x, therefore, should be less than or equal to $2(S - 1)$. For $S \leq 1$, the linear U_s - u_p form becomes unbounded only as μ approaches the infinite. In this case, Γ_x must approach zero. Similarly, for polynomial fit Hugoniots, shock pressure becomes unbounded only when compression approaches infinity. Thus, the Grüneisen coefficient Γ should also approach zero, all the while remaining less than $2/\mu$, as compressions become very large.

It is unfortunate that data for Γ are generally only available at the ambient $\mu = 0$ condition. As a result of this, it has been common practice to leave the value of Γ constant in numerical computations for lack of better data. In analyzing the data of Kohn (1969), it is observed that none of the data presented violate the Mode II stability criterion, $0 < \Gamma < 2/\mu$, for the range of μ over which the data are collected. However, should the data be extrapolated to larger values of μ, Mode II instabilities may result, since 100% of the cubic fits, and 74.5% of the linear U_s - u_p fits described by Kohn (1969) will violate Mode II stability at larger μ if Γ is held constant at its initial value.

13. CORRECTIONS FOR MODE II INSTABILITY

To enhance Mode II stability, some code developers have imposed functional forms on the Grüneisen coefficient. In the case of the EPIC codes, this is not done, and Γ is held constant at Γ_o. As pointed out, Mode II criterion will be violated for $\mu > 2/\Gamma_o$. In HULL (Matuska and Osborn 1987), the value of Γ is a defined as $\Gamma = \Gamma_o\, \rho_o/\rho$, which in terms of compression μ, is

$$\Gamma = \Gamma_o/(1 + \mu) .$$

This form can still violate the Mode II criterion if $\Gamma_o > 2$ and $\mu > 2/(\Gamma_o - 2)$. DYNA (Hallquist 1989), as well as versions of CALE (Tipton 1989), use a first order correction to Γ_o, which is equivalent to assuming the form on the Grüneisen parameter as

$$\Gamma = (\Gamma_o + A\mu)/(1 + \mu) ,$$

where A is a parameter which, when fit to EOS data at moderate pressures, is always greater than or equal to zero and generally lies in the vicinity of 0.5 for most metals (Tipton 1989). If the value of A is chosen as zero, the DYNA/CALE form for Γ reduces into that used by HULL. Even though a positive value for the parameter A might cause the data to fit better at the pressures of interest, it also has the side effect of lessening stability at larger compression. If A is positive, the limits on compression which assure Mode II stability are

$$\mu < \frac{(2 - \Gamma_o) + \left[(2 - \Gamma_o)^2 + 8A\right]^2}{2A} , \quad A > 0 .$$

For materials like aluminum, with $\Gamma_o = 2.09$ and A = 0.49, the DYNA/CALE Grüneisen form has a limiting compression of stability near 2. This value is better than the limiting value of unity, derived from the constant $\Gamma = 2$ assumption, but is still prone to failure when simulating hypervelocity impact. MESA (Bolstad 1990) uses a form:

$$\Gamma = \gamma_o + \gamma_1/(1 + \mu) ,$$

which is directly convertable into the CALE version, if one takes $\Gamma_o = (\gamma_o + \gamma_1)$ and $A = \gamma_o$. Thus, the arguments made about the CALE form apply to MESA as well.

From the perspective of assuring Mode II stability, even at very large compressions, an alternate Grüneisen form, being proposed here is given as follows:

$$\Gamma = \frac{\Gamma_o}{1 + \beta\mu} ,$$

where β is the newly introduced parameter. Unlike the other forms on Γ, where stability is a coincidental by-product of the choice of Γ_o, Mode II stability can always be ensured, with the current form, given appropriate choice of β. The form reduces to that used by HULL if β is forced to unity and can be made to approach constant Γ if β equals 0. However, constraining β to a value greater than or equal to $\Gamma_o/2$ will ensure, for any Hugoniot form, that Mode II stability is always satisfied for any finite μ. The constraint on β can be relaxed somewhat if the associated Hugoniot form is valid only in some finite range $0 \le \mu < \mu_x$. An example of such a limited domain Hugoniot is the U_s - u_p form, with $S > 1$, where $\mu_x = 1/(S - 1)$. For these cases, the constraint on β, to ensure Mode II stability, is

$$\beta \ge \frac{\Gamma_o - (2/\mu_x)}{2} .$$

To see how this proposed form can match the DYNA/CALE form at lower compressions but still provide stability at higher compressions, Figure 2 is provided. In it, three Grüneisen relationships for aluminum are shown (data for aluminum, $\Gamma_o = 2.09$, and $S = 1.33$ are extracted from Kohn [1969]). The A = .49 (CALE) curve shows the functional form of Γ, using the DYNA/CALE functional form. The value of A = .49 comes directly from the CALE manual (Tipton 1989) and was fitted from experimental data. At large compressions (in excess of 2), the CALE Grüneisen form violates Mode II stability. The A = 0 (HULL) curve shows the DYNA/CALE curve for A = 0, which reduces into the form used by HULL. This form remains stable out to the limit compression, $\mu_x = 3$, but does not follow the CALE curve well at lesser compressions, where experimental data were used to fit the A parameter. The $\beta = .72$ curve, which follows the functional form of the currently proposed model, follows the CALE curve well at lower compressions, and retains stability out to the limit compression. Notice that the minimum value of β, which is guaranteed to retain stability, can be obtained by substituting $\Gamma_o = 2.09$ and $\mu_x = 1/(1.33 - 1) = 3$ into the equation above. This minimum value is computed as 0.712, which thus guided the selection of $\beta = .72$ for the figure.

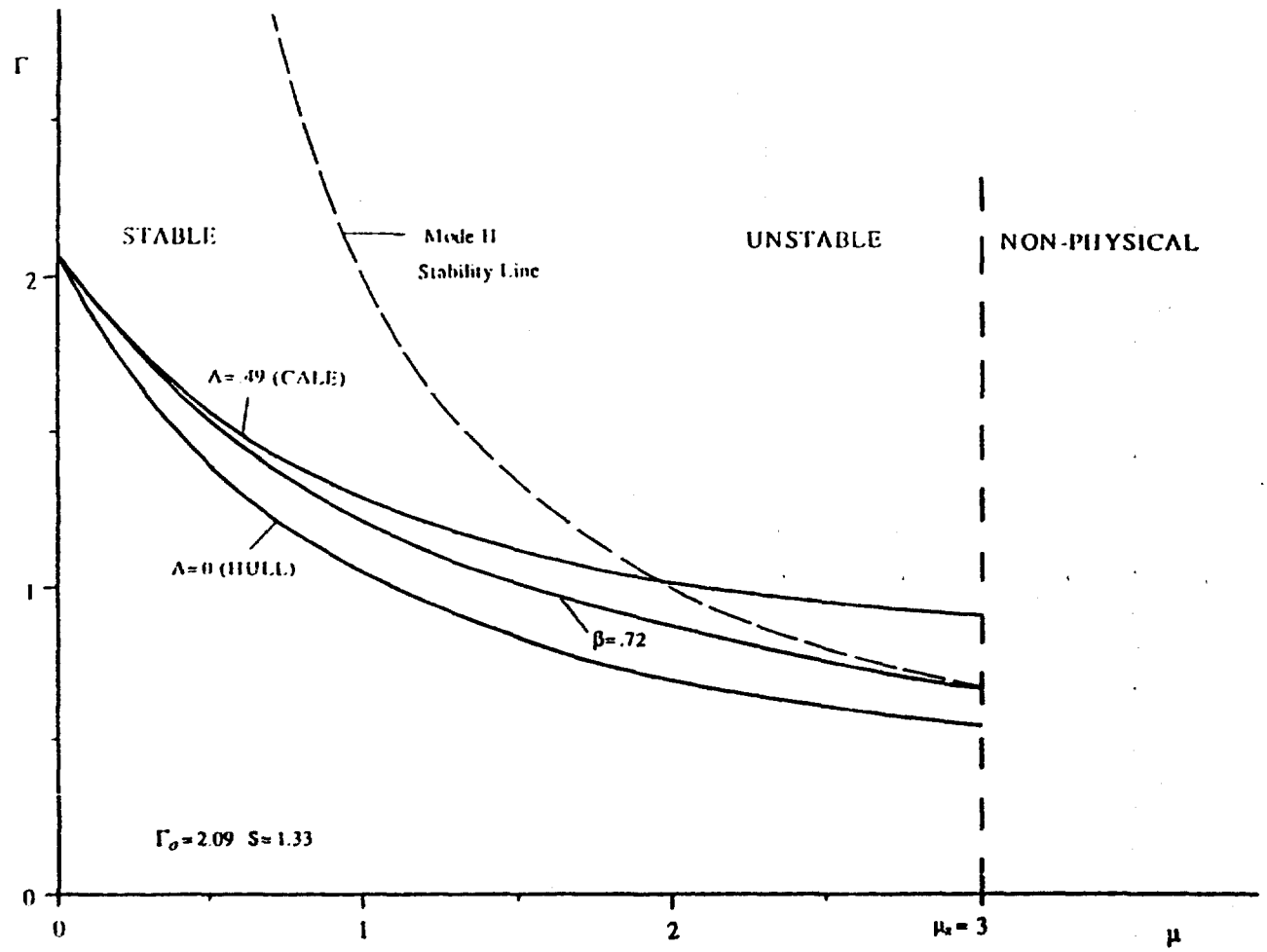

Figure 2. Comparison of Grüneisen Parameter Fits From CALE and HULL Codes for Aluminum With the Currently Proposed Fitting Model, in Light of Mode II Stability Criterion.

Note that some non-positive values of β are permissable, but only if $\Gamma_o \leq 2/\mu_x$ is true. For a polynomial Hugoniot fit, where μ_x is necessarily infinite, β is necessarily positive. One can combine the β constraint directly with the proposed Γ relation to obtain the relation in terms of Γ_o, μ_x and μ:

$$\Gamma \leq \frac{2\,\Gamma_o}{2 + (\Gamma_o - 2/\mu_x)\,\mu} .$$

14. MODE III INSTABILITY USING THE MIE-GRÜNEISEN EQUATION OF STATE

Mode III instability arises, when the square of the local speed of sound is computed as negative—a situation which clearly bears no relation to any real phenomenon. In the Mie-Grüneisen EOS, it can arise, because of the fact that the EOS is linearized about some reference curve, which is the Hugoniot, for impact computations. Since the real world is rarely linear, this idealized linearization becomes less and less accurate the further one gets from the reference curve. When one gets suitably distant from the reference curve, the thermodynamic data generated from a linearized EOS can be not only inaccurate but also in violation of basic thermodynamic principles.

When the situation of imaginary sound speed occurs, many codes (EPIC3, for example) reset their value to zero and merrily continue on their computational way. Unfortunately, the situation can be much more serious than just computing an inaccurate sonic velocity. An imaginary sonic velocity implies that an increment of isentropic compression on an element will result in a DECREASE in pressure. Resetting the sonic velocity to zero does nothing to prevent the thermodynamic state of the element from going berserk. It is these sorts of situations which most often result in catastrophic manifestations of instability over the span of one or several computational iterations—ballooning elements, collapsing elements, and wild energy fluxes are typical.

The local speed of sound is defined as the rate at which an infinitesimal disturbance propagates through a medium. Expressed by the symbol "C", it is mathematically expressed as:

$$C^2 = \partial p/\partial \rho \,|_s .$$

To derive its functional form for the Mie-Grüneisen EOS,

$$p - p_h = \Gamma \rho \, (E - E_h) \, ,$$

take the derivative with respect to an increment of density ($d\rho$) along the isentrope. This produces the following result:

$$\left. \frac{\partial p}{\partial \rho} \right|_s - \frac{dp_h}{d\rho} = \Gamma \rho \left(\left. \frac{\partial E}{\partial \rho} \right|_s - \frac{dE_h}{d\rho} \right) + (E - E_h) \, \frac{d}{d\rho} \, (\Gamma \rho) \, .$$

Converting the derivatives into compression form, this relation may be ultimately simplified, with energy terms eliminated, to produce the result:

MODE III CRITERION:

$$\rho_o \, C^2 = \left(\frac{\Gamma + 1}{1 + \mu} + \frac{1}{\Gamma} \, \frac{d\Gamma}{d\mu} \right) (p - p_h) + \frac{dp_h}{d\mu} - \frac{\Gamma}{2} \left(\mu \, \frac{dp_h}{d\mu} - \frac{p_h - p_o}{1 + \mu} \right) > 0 \, .$$

For the special case of $p = p_h$ (i.e., along the Hugoniot), this form expresses the relationship derived for Γ in Section XI,

$$\Gamma = \frac{2}{\mu} \, \frac{\left[\mu \, dp_h / d\mu - \mu \rho_o C^2 \right]}{\left[\mu \, dp_h / d\mu - (p_h - p_o) / (1 + \mu) \right]} \, ,$$

which was subsequently used to derive the Mode II criterion. Note, however, that Mode III only requires the sound speed to be positive at all thermodynamic states, whereas Mode II required the slope of the isentrope (which is directly related to the sound speed) to be not only positive but greater than the Rayleigh line slope. Thus, the Mode II criterion is more stringent than Mode III, but it only applies along a Hugoniot.

Thus, if the Mode III criterion is violated at some state, which happens to lie on the Hugoniot (ρ_h, μ), then the Mode II criterion will have already been violated at that compression μ. However,

the full Mode III criterion gives the opportunity to study stability at all states in the (p, v) or (p, μ) plane, not just along the Hugoniot.

Operational simplifications may be possible when applying the Mode III criterion, depending on the actual choices of the p_h and Γ functions. As an example, if one adopts the functional form for the Grüneisen coefficient proposed in Section XII, $\Gamma = \Gamma_o/(1 + \beta\mu)$, then the Grüneisen derivative terms simplify nicely:

$$\frac{1}{\Gamma}\frac{d\Gamma}{d\mu} = -\frac{\Gamma}{\Gamma_o}\beta = -\frac{\beta}{(1+\beta\mu)} .$$

Because of the linearized nature of Mie-Grüneisen, there can be states where Mode III stability is violated. However, their occurance can be greatly reduced, given an appropriate choice of p_h and Γ functions. As an example, consider Figure 3, which depicts the (p, v) plane cubic fit Hugoniot for aluminum with coefficients .79903, 1.13927, and 1.39792 Mbar, respectively, and density of 2.7 g/cm^3 as given in Kohn (1969). If Γ is held constant at its initial value of 2.09, corresponding to $\beta = 0$ in the currently proposed model, the Mode III stability line, which divides the (p, v) plane into stable and unstable regions, is seen to produce instability in a large part of the (p, v) plane, including thermodynamic states in which the simulation might reasonably expect to exist. Note that an isentrope, when it crosses into the unstable region of the (p, v) plane, changes its slope so that increased compressions actually cause a decrease in pressure. It is this sort of unstable behavior which will cause a simulation to come screeching to a halt in no time at all.

On the other hand, if β is increased to a value which guarantees Mode II stability, as discussed in the previous section, Mode III stability is also greatly enhanced. Since a cubic fit Hugoniot has no limiting value of compression, the value of β to guarantee Mode II stability must equal or exceed $\Gamma_o/2$, which for the case in point ($\Gamma_o = 2.09$), is 1.045. With this new value of β, shown in Figure 4, the unstable region is limited to a very small portion of the (p, v) plane, which represents material under very large tensions. In fact, the tensions required to produce instability are so large (391 kbar at $v = v_o$, for the case in point), that aluminum's spall pressure would be exceeded and material failure would occur before the material was ever able to approach this unstable thermodynamic state.

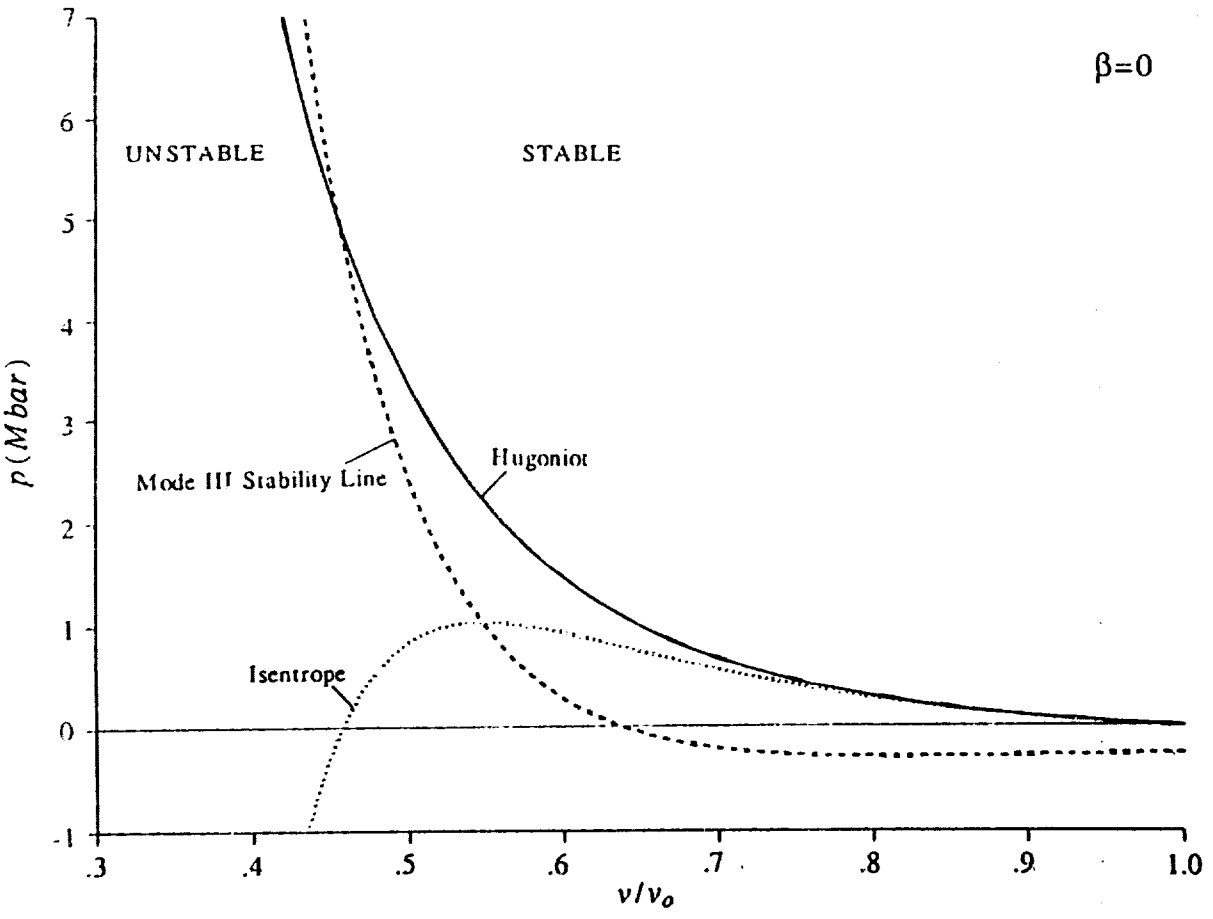

Figure 3. Depiction of Aluminum (ρ_o = 2.7) Hugoniot, Isentrope, and Mode III Stability Region for Constant Grüneisen Parameter Γ = 2.09 (β = 0). Hugoniot Is a Cubic Fit, With Parameters .79903, 1.13927, and 1.39792 Mbar, Respectively.

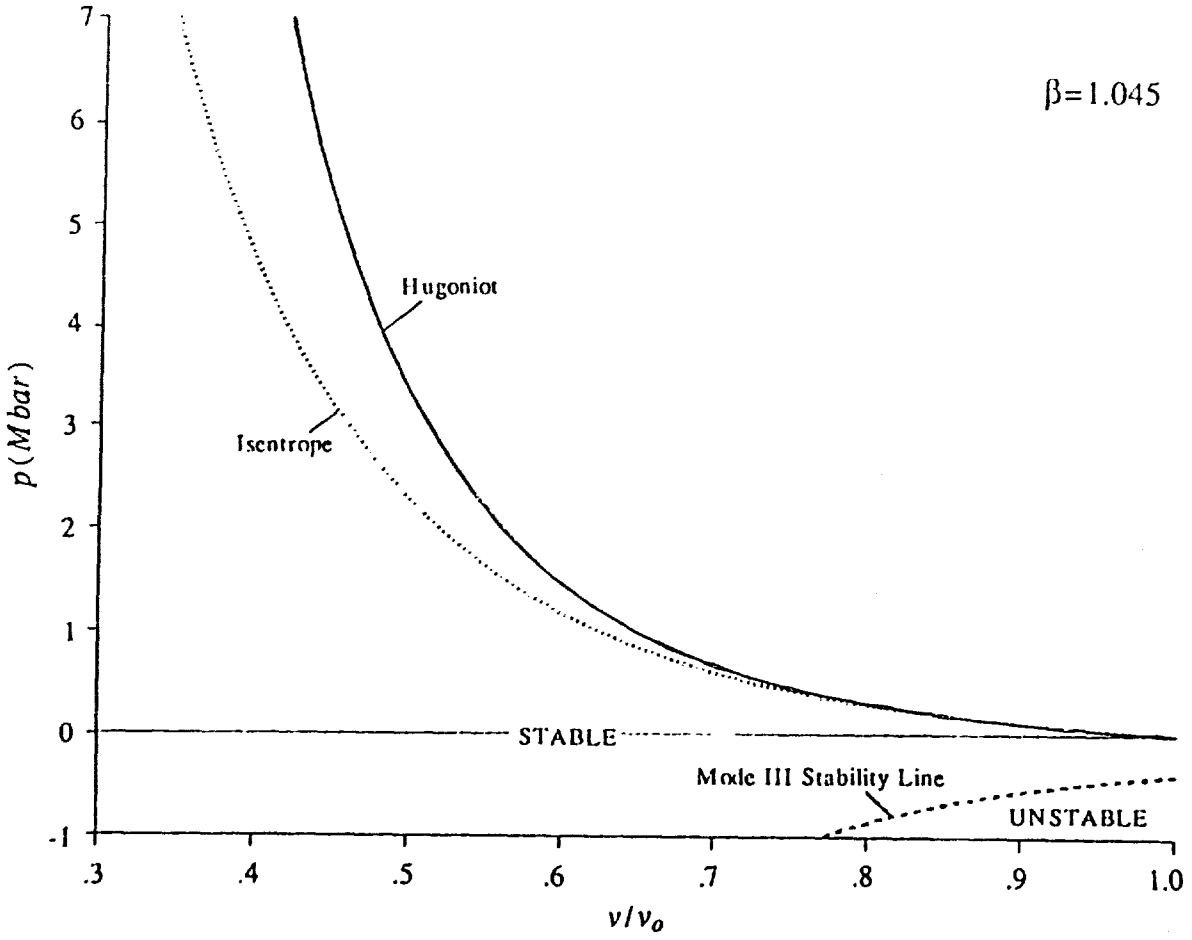

Figure 4. Depiction of Aluminum (ρ_o = 2.7) Hugoniot, Isentrope, and Mode III Stablility Region for Variable Grüneisen Parameter (β = 1.045). Hugoniot Is a Cubic Fit, With Parameters .79903, 1.13927, and 1.39792 Mbar, Respectively.

15. OTHER PROBLEMS WITH MIE-GRÜNEISEN EOS IMPLEMENTATIONS

Movement of nodes along Lagrangian contact surfaces may produce occasional values of compression in excess of that anticipated from analytical considerations. Though such artifacts are purely computational, they can cause the compression to go out of (p, v) domain of known data or, worse yet, out of the physically plausible (p, v) domain. When this happens, the code may die instantly or generate state values so inaccurate as to cause computational "ripples" which disturb the rest of the otherwise valid computation. This problem can usually be circumvented by forcing a smaller integration timestep on the computation or, alternately, by using an EOS formulation which remains physical out to larger values of compression.

16. CONCLUSIONS

A review of fundamental shock-transition theory was presented. The equation of state was introduced as an analytical vehicle to express material pressure as a function of density and temperature (or internal energy in the case of adiabatic transition). The importance of thermodynamic principles was emphasized as a tool to study the stability of various EOS implementations. The Mie-Grüneisen EOS, with a Hugoniot reference function, was singled out for study because of its relative importance in the computational modeling of shock transition.

Starting from the fundamental laws of thermodynamics, three criteria were developed to measure the stability of equations of state and were applied specifically to the Mie-Grüneisen EOS, with Hugoniot reference, to investigate the stability characteristics thereof. Results indicate numerous possibilities of instability under various circumstances. Circumstances which could bring on the investigated instabilities included: 1) an improperly formulated EOS; 2) the choice of improper data for an otherwise suitable EOS; 3) the application of given EOS data beyond the thermodynamic region for which the data were originally intended; and 4) the assumption of parameter constancy when additional data were not readily available. Several sources of published material data and Hugoniot forms were investigated for stability. Instability was observed in these data, especially so under conditions where the applied compression was greater than that for which the data were fit. Unfortunately, the existence in codes of "EOS material libraries" virtually guarantees the indiscriminate use of EOS data, thus enhancing the likelihood of EOS instability.

Based on this report's findings and the author's experience, it is believed that a significant percentage of hydrocode computations which fail do so as a direct or indirect result of the EOS calculation. Typical code failures (for example: negative absolute energies or pressures, exploding or collapsing elements, and negative element stiffnesses) are due, probably in part, if not completely, to internal inconsistencies arising from a misapplied EOS. A basic understanding of thermodynamics and its relationship to shock transition will permit the thoughtful code developer and user to verify, in advance of computational solution, the validity of his data and EOS forms.

17. REFERENCES

Bolstad, J. "MESA Generator & Generator Window Input Specifications." LA-90-131, Los Alamos National Laboratory, Los Alamos, NM, 14 March 1990.

Hallquist, J. O., and R. G. Whirley. "DYNA3D User's Manual." UCID-19592, Lawrence Livermore National Laboratory, Livermore, CA, Rev. 5, May 1989.

Johnson, G. R., D. D. Colby, and D. J. Vavrick. "Further Development of the EPIC-3 Computer Program for Three-Dimensional Analysis of Intense Impulsive Loading." AFATL-TR-78-81, Air Force Armament Laboratory, Eglin AFB, FL, July 1978.

Kohn, B. J. "Compilation of Hugoniot Equations of State." AFWL-TR-69-38, Air Force Weapons Laboratory, Kirtland AFB, NM, April 1969.

Matuska, D. A., and J. J. Osborn. "HULL Documentation." Orlando Technology, Inc. Report, Orlando, FL, Rev., May 1987.

McQuarrie, D. A. Statistical Mechanics. New York: Harper Row, 1976.

Tipton, R. "CALE User's Manual, Version 890801." Lawrence Livermore National Laboratory, Livermore, CA, 1 August 1989.

Zeldovich, Y. B., and Y. P. Razier. Physics of Shock Waves and High-Temperature Hydrodynamic Phenomena. Academic Press: New York, 1966.

Zuker, R. D. Fundamentals of Gas Dynamics. Portland: Matrix Publishers, 1977.

INTENTIONALLY LEFT BLANK.

No of Copies	Organization
2	Administrator Defense Technical Info Center ATTN: DTIC-DDA Cameron Station Alexandria, VA 22304-6145
1	HQDA (SARD-TR) WASH DC 20310-0001
1	Commander U.S. Army Materiel Command ATTN: AMCDRA-ST 5001 Eisenhower Avenue Alexandria, VA 22333-0001
1	Commander U.S. Army Laboratory Command ATTN: AMSLC-DI. 2800 Powder Mill Road Adelphi, MD 20783-1145
2	Commander U.S. Army Armament Research, Development, and Engineering Center ATTN: SMCAR-IMI-I Picatinny Arsenal, NJ 07806-5000
2	Commander U.S. Army Armament Research, Development, and Engineering Center ATTN: SMCAR-TDC Picatinny Arsenal, NJ 07806-5000
1	Director Benet Weapons Laboratory U.S. Army Armament Research, Development, and Engineering Center ATTN: SMCAR-CCB-TL Watervliet, NY 12189-4050
1	Commander U.S. Army Armament, Munitions and Chemical Command ATTN: SMCAR-ESP-L Rock Island, IL 61299-5000
1	Director U.S. Army Aviation Research and Technology Activity ATTN: SAVRT-R (Library) M/S 219-3 Ames Research Center Moffett Field, CA 94035-1000

No of Copies	Organization
1	Commander U.S. Army Missile Command ATTN: AMSMI-RD-CS-R (DOC) Redstone Arsenal, AL 35898-5010
1	Commander U.S. Army Tank-Automotive Command ATTN: AMSTA-TSL (Technical Library) Warren, MI 48397-5000
1	Director U.S. Army TRADOC Analysis Command ATTN: ATRC-WSR White Sands Missile Range, NM 88002-5502
(Class. only)1	Commandant U.S. Army Infantry School ATTN: ATSH-CD (Security Mgr.) Fort Benning, GA 31905-5660
(Unclass. only)1	Commandant U.S. Army Infantry School ATTN: ATSH-CD-CSO-OR Fort Benning, GA 31905-5660
1	Air Force Armament Laboratory ATTN: AFATL/DLODL Eglin AFB, FL 32542-5000
	Aberdeen Proving Ground
2	Dir, USAMSAA ATTN: AMXSY-D AMXSY-MP, H. Cohen
1	Cdr, USATECOM ATTN: AMSTE-TD
3	Cdr, CRDEC, AMCCOM ATTN: SMCCR-RSP-A SMCCR-MU SMCCR-MSI
1	Dir, VLAMO ATTN: AMSLC-VL-D
10	Dir, BRL ATTN: SLCBR-DD-T

No. of Copies Organization

2 Director
DARPA
ATTN: J. Richardson
MAJ R. Lundberg
1400 Wilson Blvd.
Arlington, VA 22209-2308

1 Defense Nuclear Agency
ATTN: MAJ James Lyon
6801 Telegraph Rd.
Alexandria, VA 22192

1 Commander
US Army Strategic Defense Command
ATTN: CSSD-H-LL, Tim Cowles
Huntsville, AL 35807-3801

1 Commander
USA ARMC
ATTN: ATSB-CD, Dale Stewart
Ft. Knox, KY 40121

1 Commander
US Army MICOM
ATTN: AMSMI-RD-TE-F, Matt H. Triplett
Redstone Arsenal, AL 35898-5250

2 Commander
TACOM RD&E Center
ATTN: AMCPM-ABMS-SA, John Rowe
AMSTA-RSS, K. D. Bishnoi
Warren, MI 48397-5000

2 Commander
US Army, ARDEC
ATTN: SMCAR-CCH-V, M. D. Nicolich
SMCAR-FSA-E, W. P. Dunn
Picatinny Arsenal, NJ 07806-5000

4 Commander
US Army Belvoir RD&E Center
ATTN: STRBE-NAE, Bryan Westlich
STRBE-JMC, Terilee Hanshaw
STRBE-NAN, Steven G. Bishop
STRBE-NAN, Josh Williams
Ft. Belvoir, VA 22060-5166

No. of Copies Organization

1 USMC/MCRDAC/PM Grounds Wpns. Br.
ATTN: Dan Haywood
Firepower Div.
Quantico, VA 22134

3 Commander
Naval Weapons Center
ATTN: Tucker T. Yee (Code 3263)
Don Thompson (Code 3268)
W. J. McCarter (Code 6214)
China lake, CA 93555

2 Commander
Naval Weapons Support Center
ATTN: John D. Barber
Sung Y. Kim
Code 2024
Crane, IN 47522-5020

3 Commander
Naval Surface Warfare Center
ATTN: Charles R. Garnett (Code G-22)
Linda F. Williams (Code G-33)
Mary Jane Sill (Code H-11)
Dahlgren, VA 22448-5000

11 Commander
Naval Surface Warfare Center
ATTN: Pao C. Huang (G-402)
Bryan A. Baudler (R-12)
Robert H. Moffett (R-12)
Robert Garrett (R-12)
Thomas L. Jungling (R-32)
Richard Caminity (U-43)
John P. Maira
Paula Walter
Lisa Mensi
Kenneth Kiddy
F. J. Zerilli
10901 New Hampshire Ave.
Silver Spring, MD 20903-5000

1 Director
Naval Civil Engr. Lab.
ATTN: Joel Young (Code L-56)
Port Hueneme, CA 93043

No. of
Copies Organization

4 Air Force Armament Laboratory
ATTN: AFATL/DLJW (W. Cook)
AFATL/DLJW (M. Nixon)
AFATL/MNW (LT Donald Lorey)
AFATL/MNW (Richard D. Guba)
Eglin AFB, FL 32542

8 Director
Sandia National Laboratories
ATTN: Robert O. Nellums (Div. 9122)
Jim Hickerson (Div. 9122)
Marlin Kipp (Div. 1533)
Allen Robinson (Div. 1533)
Wm. J. Andrzejewski (Div. 2512)
Don Marchi (Div. 2512)
R. Graham (Div. 1551)
R. Lafarge (Div. 1551)
P. O. Box 5800
Albuquerque, NM 87185

8 Director
Los Alamos National Laboratory
ATTN: G. E. Cort (MS K574)
Tony Rollett (MS K574)
Mike Burkett (MS K574)
Robert Karpp (MS P940)
Rudy Henninger (MS K557, N-6)
Roy Greiner (MS-G740)
James P. Ritchie (B214, T-14)
John Bolstad (MS G787)
P. O. Box 1663
Los Alamos, NM 87545

13 Director
Lawrence Livermore National Laboratory
ATTN: Barry R. Bowman (L-122)
Ward Dixon (L-122)
Raymond Pierce (L-122)
Russell Rosinsky (L-122)
Owen J. Alford (L-122)
Diana Stewart (L-122)
Tony Vidlak (L-122)
Albert Holt (L-290)
John E. Reaugh (L-290)
David Wood (L-352)
Robert M. Kuklo (L-874)
Thomas McAbee (MS-35)
Michael J. Murphy
P. O. Box 808
Livermore, CA 94550

No. of
Copies Organization

1 Battelle Northwest
ATTN: John B. Brown, Jr.
MSIN 3 K5-22
P. O. Box 999
Richland, WA 99352

1 Advanced Technology, Inc.
ATTN: John Adams
P. O. Box 125
Dahlgren, VA 22448-0125

1 Explosive Technology
ATTN: Michael L. Knaebel
P. O. Box KK
Fairfield, CA 94533

1 Rockwell Missile Systems Div.
ATTN: Terry Neuhart
1800 Satellite Blvd.
Duluth, GA 30136

1 Rockwell Intl./Rocketdyne Div.
ATTN: James Moldenhauer
6633 Canoga Ave (HB 23)
Canoga Park, CA 91303

2 McDonnell Douglas Helicopter
ATTN: Loren R. Bird
Lawrence A. Mason
5000 E. McDowell Rd. (MS 543-D216)
Mesa, AZ 85205

1 University of Colorado
Campus Box 431 (NNT 3-41)
ATTN: Timothy Maclay
Boulder, CO 80309

1 New Mexico Inst. Mining & Tech.
Campus Station (TERA Group)
ATTN: David J. Chavez
Socorro, NM 87801

2 Schlumberger Perforating & Test
ATTN: Manuel T. Gonzalez
Dan Markel
P. O Box 1590/14910 Ariline Rd.
Rosharon, TX 77583-1590

No. of Copies Organization

2 Aerojet Ordnance/Exp. Tech. Ctr.
ATTN: Patrick Wolf
Gregg Padgett
1100 Bulloch Blvd.
Socorro, NM 87801

2 Physics International
ATTN: Ron Funston
Lamont Garnett
2700 Merced St./P. O. Box 5010
San Leandro, CA 94577

2 Lockheed Missile & Space Co., Inc.
ATTN: S. Kusumi (O-81-11, Bldg. 157)
Jack Philips (O-54-50)
P. O. Box 3504
Sunnyvale, CA 94088

1 Lockheed Missile & Space Co., Inc.
ATTN: Richard A. Hoffman
Santa Cruz Fac./Empire Grade Rd.
Santa Cruz, CA 95060

1 Boeing Corporation
ATTN: Thomas M. Murray (MS-84-84)
P. O. Box 3999
Seattle, WA 98124

2 Mason & Hanger - Silas Mason Co.
ATTN: Thomas J. Rowan
Christopher Vogt
Iowa Army Ammunition Plant
Middletown, IA 52638-9701

1 Nuclear Metals Inc.
ATTN: Jeff Schreiber
2229 Main St.
Concord, MA 01742

1 Lockheed Engineering & Space Sciences
ATTN: Ed Cykowski, MS B-22
2400 NASA Road 1
Houston, TX

2 Dyna East Corporation
ATTN: P. C. Chou
R. Ciccarelli
3201 Arch St.
Philadelphia, PA 19104

No. of Copies Organization

2 Southwest Research Institute
ATTN: C. Anderson
A. Wenzel
6220 Culebra Road
P. O. Drawer 28510
San Antonio, TX 78284

2 Battelle - Columbus Laboratories
ATTN: R. Jameson
S. Golaski
505 King Avenue
Columbus, OH 43201

3 Alliant Techsystems, Inc.
ATTN: Gordon R. Johnson
Tim Holmquist
Kuo Chang
MN 48-2700
7225 Northland Dr.
Brooklyn Park, MN 55428

1 S-Cubed
ATTN: R. Sedgwick
P.O. Box 1620
La Jolla, CA 92038-1620

2 California Research and Technology, Inc.
ATTN: Roland Franzen
Dennis Orphal
5117 Johnson Dr.
Pleasanton, CA 94566

2 Orlando Technology, Inc.
ATTN: Dan Matuska
J. Osborn
P. O. Box 855
Shalimar, FL 32579

3 Kaman Sciences Corporation
ATTN: D. Barnette
D. Elder
P. Russell
P. O. Box 7463
Colorado Spring, CO 80933

No. of Copies | Organization

2 Defense Research Establishment Suffield
ATTN: Chris Weickert
David MacKay
Ralston, Alberta, TOJ 2NO Ralston
CANADA

1 Defense Research Establishment Valcartier
ATTN: Norbert Gass
P. O. Box 8800
Courcelette, PQ, GOA 1RO
CANADA

1 Canadian Arsenals, LTD
ATTN: Pierre Pelletier
5 Montee des Arsenaux
Villie de Gardeur, PQ, J5Z2
CANADA

1 Ernst Mach Institute
ATTN: A. J. Stilp
Eckerstrasse 4
D-7800 Freiburg i. Br.
GERMANY

3 IABG
ATTN: H. J. Raatschen
W. Schittke
F. Scharppf
Einsteinstrasse 20
D-8012 Ottobrun B. München
GERMANY

1 Royal Armament R&D Establishment
ATTN: Ian Cullis
Fort Halstead
Sevenoaks, Kent TN14 7BJ
ENGLAND

1 Centre d'Etudes de Gramat
ATTN: SOLVE Gerard
46500 Gramat
FRANCE

1 Centre d'Etudes de Vaujours
ATTN: PLOTARD Jean-Paul
Boite Postale No. 7
77181 Country
FRANCE

No. of Copies | Organization

1 PRB S.A.
ATTN: M. Vansnick
Avenue de Tervueren 168, Bte. 7
Brussels, B-1150
BELGIUM

1 AB Bofors/Ammunition Division
ATTN: Jan Hasslid
BOX 900
S-691 80 Bofors
SWEDEN

INTENTIONALLY LEFT BLANK.